出國報告(出國類別：國際會議)

2011 美國機械工程壓力容器與管線研討會出席報告

服務機關：國立中興大學環境保育季防災科技研究中心
姓名職稱：張長菁 博士後研究員
派赴國家：美國
出國期間：20110717-20110721
報告日期：20110731

摘要

美國機械工程壓力容器與管線研討會(ASME Pressure V essels and Piping Conference)爲每年舉辦一次之大型世界會議，本屆於 2011 年 7 月 17-21 日在美國馬里蘭州巴爾的摩 Marriott Waterfront Hotel 舉行，有來自美國、日本、歐洲及全世界各地之專家學者共同參與，由美國機械工程師學會(American Society of Mechanical Engineers)主辦。本會議在地震工程-減震科技研究(Earthquake Engineering - Technology for Seismic Mitigation) 議程中集合了全球從事地震工程相關之專家學者討論地震特性、結構受震動態行爲、結構最新耐震技術以及消能減振裝置應用於土木工程結構之可行性與效用評估之最新技術與研究成果，爲地震工程領域受肯定的國際會議。本人出席本研討會並發表研究成果「H_∞ DIRECT OUTPUT FEEDBACK CONTROL OF HIGH-SPEED ELEVATOR SYSTEMS」，本報告內容主要爲出席 ASME, 2011 PVP 研討會之目的、過程、心得及建議。

目次

1. 參加 2011PVP 目的

美國機械工程壓力容器與管線研討會(ASME Pressure V essels and Piping Conference)爲每年舉辦一次之大型世界會議，本屆於 2011 年 7 月 17-21 日在美國馬里蘭州巴爾的摩 Marriott Waterfront Hotel 舉行，有來自美國、日本、歐洲及全世界各地之專家學者共同參與，由美國機械工程師學會(American Society of Mechanical Engineers)主辦。本會議在地震工程-減震科技研究(Earthquake Engineering - Technology for Seismic Mitigation) 議程中集合了全球從事地震工程相關之專家學者討論地震特性、結構受震動態行爲、結構最新耐震技術以及消能減振裝置應用於土木工程結構之可行性與效用評估之最新技術與研究成果，爲地震工程領域受肯定的國際會議，議題包括相當廣泛，主要議題計有：

1. Seismic Evaluation of Systems, Structures and Components
2. Structural Dynamics (linear and nonlinear)
3. Experimental and Analytical Studies in Systems Interaction
4. Systems Identification and Control
5. Seismic Isolation and Energy Absorbing Systems
6. Seismic Behaviour of Storage Tanks and Associated Equipment
7. Seismic Design of Piping Systems
8. Forum on Dynamic Response Behavior of Piping
9. Seismic Issues in New Reactor Licensing Activities
10. Earthquake Damages in Power Plants

此外本次還包含其他特殊領域議題，包含領域相當廣泛，共分 180 個場次。本次研討會主要目的除了發表本人今年度研究成果「H_∞ DIRECT OUTPUT FEEDBACK CONTROL OF HIGH-SPEED ELEVATOR SYSTEMS」，更希望藉此機會與國際上相關領域學者交換意見，有助於友誼交流和資訊的獲得，提升未來研究成果之水準。

2. 參加 2011PVP 過程

大會活動從 7 月 17 日下午辦理報到，本會議除了 18 日至 21 日正常論文發表會議外，並由大會邀請國際知名專家學者講演，安排專題演講，同時，主辦單位在會場中並安排了產品展示，以增加與會人員及產業界之交流。與會論文有來自中、美、日、英、義等各國 700 多篇文章，以口頭報告方式發表，參加人數在 1000 人以上，國內除本人外，尚有工研院、逢甲大學之教授及學生等 10 多位產學研界人士多人參加，本人經由國科會補助搭長榮班機於 7 月 16 日抵達美國紐華克機場，再轉搭巴士前往巴爾的摩。本人發表之論文爲「H_∞ DIRECT OUTPUT FEEDBACK CONTROL OF HIGH-SPEED ELEVATOR SYSTEMS」，於 7 月 19 日早上 8 點半發表報告，進行報告其間有多人提出問題討論，研究成果得到與會學者專家的認同與興趣，會程相當緊湊、充實。

3. 參加 2011PVP 心得及建議

參加此次會議的全球 1000 多位專家學者具有各種不同專長及專業背景，大家就共通問題交換意見，場面熱烈，獲益良多。地震迄今仍是不可預知的天然外力，對土木工程及民生設施結構的安全威脅最大，尤其是位處環太平洋地震帶的臺灣、日本及美國所受影響更深。爲保障與提昇人類居住環境及民生設施結構的安全，藉由消能減振系統及結構控制理論及技術，降低地震引起的結構動態反應，近年來廣獲專家學者研究的興趣及肯定。國內外各大工程研究機構在近年來已投入相當大的人力、物力、財力，靠其固有精湛的製造技術將各種研究成果製成實體，實際應用於高塔、建築物、橋樑等結構物上，經由試驗室振動臺試驗以及實體觀測結果確能降低地震所引起的動態反應。在本次會議中，各國從事相關專家學者發表多年研究經驗與成果，國外理論與實際充份結合的作法值得我們效法與借鏡。

感謝國立中興大學、教育部及國科會給予本人財力補助得以參加此次會議，除發表個人研究成果外，並有機會和國際上相關領域學者交換意見，有助於友誼交流和資訊的獲得，對本人未來研究助益甚大，也讓外人親身了解國內的研究成果。期盼教育部或國科會應多資助研究人員參加國際會議，增加交流學習的機會。

4. 研討會相關照片

照片 1.　研討會秩序手冊封面

照片 2.　100 年 7 月 18-21 日, 報到會場、報告、會場廠商展示並與本校土木系林其璋教授合影、及逢甲大學教授報告之照片。

Proceedings of the ASME 2011 Pressure Vessels & Piping Division Conference
PVP2011
July 17-21, 2011, Baltimore, Maryland, USA

PVP2011-57814

H∞ DIRECT OUTPUT FEEDBACK CONTROL OF HIGH-SPEED ELEVATOR SYSTEMS

Chang-Ching Chang
Post-Doctoral Research Fellow
Center for Environmental Restoration & Disaster Reduction
National Chung Hsing University
Taichung, Taiwan 40227, R.O.C.
Tel: 886-4-22862181, Fax: 886-4-22851992
Email: d9262102@mail.nchu.edu.tw

Chi-Chang Lin
Distinguished Professor
Department of Civil Engineering
National Chung Hsing University
Taichung, Taiwan 40227, R.O.C.
Tel: 886-4-22840438 ext 225, Fax: 886-4-22851992
Email: cclin3@dragon.nchu.edu.tw

Wu-Chung Su
Professor
Department of Electrical Engineering
National Chung Hsing University
Taichung, Taiwan 40227, R.O.C.
Email: wcsu@nchu.edu.tw

Yuan-Po Huang
Graduate Student
Department of Civil Engineering
National Chung Hsing University
Taichung, Taiwan 40227, R.O.C.

ABSTRACT

The more the development of super high-rise buildings, the faster the speed of elevator in order to shorten the riding time of elevator and the waiting time of passengers. With the increase of elevator speed, the horizontal vibration of passenger car becomes more significant resulting in the decrease of serviceability and safety of elevator, and the discomfort of passengers. The horizontal vibration is mainly generated from the elevator wheels running on rough and winding guide rails. In this paper, a four degree-of-freedom (DOF) elevator system was established to examine the characteristics of the excitations and to analyze the dynamic responses of the elevator. An active mass driver (AMD) was developed to reduce the horizontal acceleration of passenger car in the elevator based on H_∞ direct output feedback control algorithm. The optimal control force is obtained from the multiplication of direct output measurements by a pre-calculated time-invariant gain matrix. To achieve optimal control performance, the strategy to select both control parameters γ and α was investigated extensively. Numerical verification results show that decrease in γ or increase in α yields better control performance with an acceptable magnitude of control force. The selective ranges of γ and α making a controlled system become overdamped or unstable were found. To assure system stability and control efficiency, the upper bound of α were derived and illustrated graphically. An optimum design flowchart was also proposed. Finally, a full-scaled high-speed elevator system was investigated to prove the applicability and control effectiveness of the proposed AMD system.

KEYWORDS: High-speed elevator, active mass driver H_∞ direct output feedback control.

INTRODUCTION

The more the development of super high-rise buildings, the faster the speed of elevators is demanded in order to shorten elevator waiting and riding time. The horizontal vibration becomes more significant with the increase of the elevator speed and will decrease the serviceability, the comfort of passenger and the safety of elevator. The horizontal vibration is generated by the excitation of elevator car due to the roughness and winding of the guide rails and the turbulent flow induced by high-speed movement of the elevator.

The growing number of high-rise buildings has expedited the demand of elevator running speed for the past 20 to 30 years. As depicted in Fig. 1, the running speed of elevators has been progressing from 488mpm in the 1970's to 1,000mpm nowadays. For example, the elevator in the Taipei Financial Center (Taipei 101 building), manufactured by Toshiba Elevator and Building Systems Co., can speed up to 1,010mpm. Moreover, in addition to transporting passengers to the destination floors swiftly and safely, a high-speed elevator system should also provide a comfortable ride with least

possible vibrations. As the traveling speed of elevators become higher and higher, the vibration problem becomes even more significant than ever considered. It not only incurs comfort and safety concerns, but also shortens the lifespan of the elevator system. To reduce vibrations throughout the elevator motions has now become an imperative issue to the elevator industry.

The study of vibration control for high-speed elevator systems has not received sufficient attention yet in the literature. The Hitachi Elevator Asia Pte. Ltd. constructed a research tower of 203-meter in height to launch a high-speed elevator research project. Elevators with traveling speed up to 1,300mpm have been manufactured and implemented since 2009. In recent, China has a great demand on building elevators due to its fast growth of newly developed metropolitans. The Chinese elevator industry has put forward an extensive study on the vibration control of elevators. Quite a few research results were obtained in the literature.

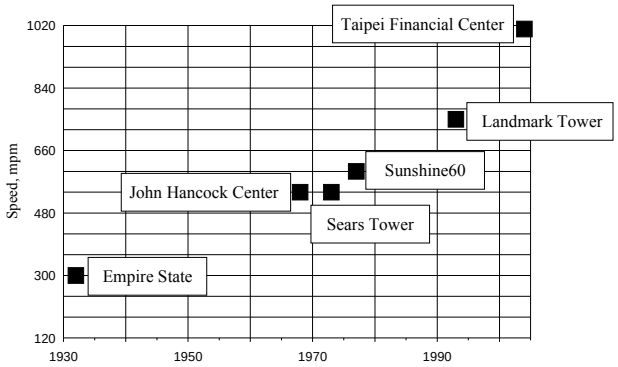

Fig. 1 History of the High-Speed Elevator

The elevator vibration can be categorized into two classes; namely, the vertical vibrations and the horizontal vibrations which are caused by the guide rail installation errors, rail surface roughness, rail curvature and deformation, roller guide defects, and airflow turbulence during transportation, and so on [2-3]. In present, there are more researches on the solution of vertical vibration problems. These results have provided a sound theoretical basis to the design and improvement of elevator's mechanical system.

On the horizontal vibration problems, Fu *et al.* [4, 5] utilized the simulation packages of Automatic Dynamic Analysis of Mechanical Systems (ADAMS) to analyze the horizontal vibration of elevator car. They found that the horizontal vibration frequencies of elevator system lie in the range of 0-15 Hz, which is human-susceptible. Once a resonance occurs in this vibration frequency range, the riders are liable to feel uncomfortable. Li *et al.* [6,7] established a two degree-of-freedom (DOF) model to study the guide rail effects in horizontal vibration. The elevator frame and the elevator car were separated from each other with rubber cushions. Such an arrangement enables a simplified 2-DOF analysis with the cost of accuracy. Okamoto *et al.* [8-9] proposed three typical external force patterns applying to the guide rails. They are the sinusoidal pattern, the triangular pattern, and the staircase pattern, respectively. Such external forces are mainly due to rail surface roughness. In this paper, in addition to the above three patterns, we will also include the impulse force pattern into the analysis of external forces on the guide rails.

The installment of guide rails with perfect measures and alignment can indeed reduce the horizontal vibrations substantially. However, in order to moderate the manufacture and the installation costs, vibration control mechanism is in effect a preferred approach. The structural vibration control techniques have been proven to be very useful in compensating the disturbances due to winds and earthquakes. They have also been successfully implemented in reducing the horizontal vibrations of high rise buildings, towers, and suspension bridges.

The passive control approaches as such do not require additional external energy source. They are structurally simple, robust, easy to realize, and more cost effective. However, these passive control approaches are also liable to the time-varying external disturbances. The stability margin is usually limited to the intrinsic features of the structure and can hardly been improved as the building gets higher and elevator speeds get faster. However, the active control approaches provides additional flexibilities in coping with the external vibration sources. In particular, the external vibration sources are time-varying functions. Instantaneous measurements are therefore very important in computing the active control forces in response to those external disturbances.

The research on active control of high-speed elevator is still a barren area in the literature. To name just a few, Skalski *et al*. [10] practiced active control in dealing with horizontal vibration problems. They used electromechanical drive systems to reduce the horizontal acceleration of elevator car. In addition, the active mass driver (AMD) manufactured by the Hitachi Elevator Asia Pte. Ltd. has proven to be successful. The research on vibration control of high-speed elevator is obviously still in need.

The purpose of this paper is to develop an active mass driver (AMD) control system to reduce the horizontal vibration of passenger car during the operation of elevator. First, a four-DOF dynamic model of elevator was established to examine the characteristics of the excitations and to analyze the dynamic responses of the elevator. A robust H_∞ control strategy is applied to calculate the optimal control force based on direct output measurements. Finally, numerical verifications from a full-scaled high-speed elevator system were conducted to assure the control effectiveness of the proposed AMD control system.

VIBRATION ANALYSIS OF ELEVATOR SYSTEMS

Overview of Elevator Systems

Fig. 2 shows a diagram of an elevator system. It consists of elevator car structure and guide system. An elevator car is mainly composed of a car cabin and a car frame. Isolation rubbers are installed between the cabin and the frame. Four roller guide units which hold three roller guides facing the guide rail in three directions are fixed at the four corners of car frame. The elevator car goes up and down along two guide rails

which are fixed to the hoist way as straightly as possible. Installation accuracy of guide rails influences the riding characteristics. Each roller consists of a lever, a spring, and a damper to absorb vibrations when the car goes over deformed rails.

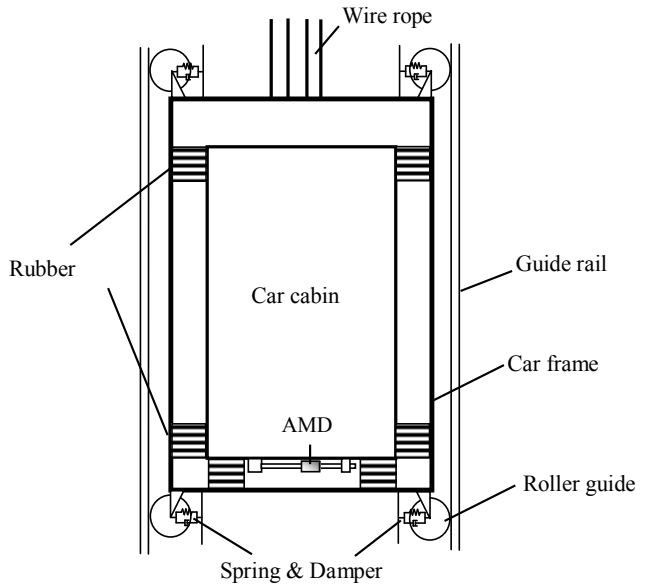

Fig. 2 Elevator System

Loading Type for Horizontal Vibration of Elevator Systems

It is generally recognized that the surface roughness of guide rail, rail bending and distortion, and the associated aligning errors in the process of installation are the major causes of horizontal vibration of the car cabin when the elevator system is in operation [9]. Let $x_{w,bending}$ be bending deformation, $x_{w,step}$ be stepwise deformation, and $x_{w,skew}$ be skew deformation of the guide rails. Assuming that the left and the right rails have the same deformation patterns, the rail deformations can then be described as functions of building height, *h*, as follows:

$$x_{w,bending}(h) = \delta_{\max} \cdot \sin\left(2\pi \cdot \frac{h}{2L}\right) \tag{1a}$$

$$x_{w,step}(h) = \begin{cases} \delta_{\max} & , \text{ if } 0 \le R < L \\ -\delta_{\max} & , \text{ if } L \le R < 2L \end{cases} \tag{1b}$$

$$x_{w,skew}(h) = \begin{cases} \dfrac{R}{L}\delta_{\max} & , \text{ if } 0 \le R < L \\ -\dfrac{2L-R}{L}\delta_{\max} & , \text{ if } L \le R < 2L \end{cases} \tag{1c}$$

where $\delta_{\max}$ is the maximum deformation. L is the unit rail length. $R = \mathrm{rem}(h/2L)$ is the remainder of the building height divided by two times of the rail length.

Dynamic Equations of Motion of Elevator-AMD Systems

It is reasonably assumed that the car cabin and car frame are two rigid bodies. Only their horizontal translation and rotation motions are considered. Define the variables x_c and θ_c as the horizontal displacement and rotational angle of the center of car cabin. Similarly, x_f, θ_f as the horizontal displacement and rotational angle of the center of car frame. Also define the disturbance variables x_{w1}, x_{w2}, x_{w3}, and x_{w4} as the displacements at the respective roller guide parts due to the rail winding. Thus, the dynamic equations of motion for the car cabin and car frame take the following four forms as

$$\begin{aligned} & m_c\ddot{x}_c + (2c_1 + 2c_2)\dot{x}_c + (2k_1 + 2k_2)x_c \\ & + (-2l_{c1}c_1 + 2l_{c2}c_2)\dot{\theta}_c + (-2l_{c1}k_1 + 2l_{c2}k_2)\theta_c \\ & - (2c_1 + 2c_2)\dot{x}_f - (2k_1 + 2k_2)x_f \\ & + (2l_{f1}c_1 - 2l_{f2}c_2)\dot{\theta}_f + (2l_{f1}k_1 - 2l_{f2}k_2)\theta_f = 0 \end{aligned} \tag{2a}$$

$$\begin{aligned} & I_c\ddot{\theta}_c + (-2l_{c1}c_1 + 2l_{c2}c_2)\dot{x}_c + (-2l_{c1}k_1 + 2l_{c2}k_2)x_c \\ & + (2l_{c1}^2c_1 + 2l_{c2}^2c_2 + 2l_3^2c_3)\dot{\theta}_c \\ & + (2l_{c1}^2k_1 + 2l_{c2}^2k_2 + 2l_3^2k_3)\theta_c \\ & + (2l_{c1}c_1 - 2l_{c2}c_2)\dot{x}_f + (2l_{c1}k_1 - 2l_{c2}k_2)x_f \\ & - (2l_{c1}l_{f1}c_1 + 2l_{c2}l_{f2}c_2 + 2l_3^2c_3)\dot{\theta}_f \\ & - (2l_{c1}l_{f1}k_1 + 2l_{c2}l_{f2}k_2 + 2l_3^2k_3)\theta_f = 0 \end{aligned} \tag{2b}$$

$$\begin{aligned} & m_f\ddot{x}_f + (-2c_1 - 2c_2)\dot{x}_c + (-2k_1 - 2k_2)x_c \\ & + (2l_{c1}c_1 - 2l_{c2}c_2)\dot{\theta}_c + (2l_{c1}k_1 - 2l_{c2}k_2)\theta_c \\ & + (-2l_{f3}c_{r1} + 2l_{f4}c_{r2} - 2l_{f1}c_1 + 2l_{f2}c_2)\dot{\theta}_f \\ & + (-2l_{f3}k_{r1} + 2l_{f4}k_{r2} - 2l_{f1}k_1 + 2l_{f2}k_2)\theta_f \\ & + (2c_{r1} + 2c_{r2} + 2c_1 + 2c_2)\dot{x}_f \\ & + (2k_{r1} + 2k_{r2} + 2k_1 + 2k_2)x_f \\ & = c_{r1}(\dot{x}_{w1} + \dot{x}_{w3}) + c_{r2}(\dot{x}_{w2} + \dot{x}_{w4}) \\ & + k_{r1}(x_{w1} + x_{w3}) + k_{r2}(x_{w2} + x_{w4}) \end{aligned} \tag{2c}$$

$$\begin{aligned} & I_f\ddot{\theta}_f + 2(l_{f1}c_1 - l_{f2}c_2)\dot{x}_c + 2(l_{f1}k_1 - l_{f2}k_2)x_c \\ & + 2(l_{f3}^2c_{r1} + l_{f4}^2c_{r2} + l_{f1}^2c_1 + l_{f2}^2c_2 + l_3^2c_3)\dot{\theta}_f \\ & + 2(l_{f3}^2k_{r1} + l_{f4}^2k_{r2} + l_{f1}^2k_1 + l_{f2}^2k_2 + l_3^2k_3)\theta_f \\ & + 2(-l_{f3}c_{r1} + l_{f4}c_{r2} - l_{f1}c_1 + l_{f2}c_2)\dot{x}_f \\ & + 2(-l_{f3}k_{r1} + l_{f4}k_{r2} - l_{f1}k_1 + l_{f2}k_2)x_f \\ & + 2(-l_{c1}l_{f1}c_1 - l_{c2}l_{f2}c_2 - l_3^2c_3)\dot{\theta}_c + \\ & 2(-l_{c1}l_{f1}k_1 - l_{c2}l_{f2}k_2 - l_3^2k_3)\theta_c \\ & = -l_{f3}c_{r1}(\dot{x}_{w1} + \dot{x}_{w3}) + l_{f4}c_{r2}(\dot{x}_{w2} + \dot{x}_{w4}) \\ & - l_{f3}k_{r1}(x_{w1} + x_{w3}) + l_{f4}k_{r2}(x_{w2} + x_{w4}) \end{aligned} \tag{2d}$$

where m_c = mass of car cabin, I_c = mass moment of inertia of car cabin, m_f = mass of car frame, I_f = mass moment of

inertia of car frame; As shown in Fig. 3, l_{c1} and l_{c2} are the vertical distances of the center of mass (COM) of car cabin to the upper rubbers and the lower rubbers of car cabin, respectively. Similarly, l_{f1}, and l_{f2} are the vertical distances from the COM of car frame to the upper rubbers and the lower rubbers of car frame. l_3 is the horizontal distance from rubber to the COM of car cabin. l_{f3} and l_{f4} are the vertical distances from the two rollers guides to the COM of car frame. k_{r1}, k_{r2}, c_{r1}, and c_{r2} are the spring constants and the damping coefficients of the upper and lower roller guides. The spring constants and the damping coefficients for the two horizontal and one vertical rubbers are k_1, k_2, k_3, and c_1, c_2, c_3, respectively.

Consider the above 4-DOF elevator system equipped with an active mass driver (AMD) at the bottom of car cabin as shown in Fig. 1. The control force $\boldsymbol{u}(t)$ is expressed as

$$\boldsymbol{u}(t) = m_{AMD}\ddot{x}_{AMD} \tag{3}$$

where m_{AMD} and $\ddot{x}_{AMD}$ are the mass and acceleration of active driver. Then, the equations of motion of the combined elevator-AMD system can be rewritten in matrix form as

$$\boldsymbol{M}\ddot{\boldsymbol{x}}(t) + \boldsymbol{C}\dot{\boldsymbol{x}}(t) + \boldsymbol{K}\boldsymbol{x}(t) = \boldsymbol{B}_1\boldsymbol{u}(t) + \boldsymbol{E}_1\boldsymbol{w}(t) \tag{4}$$

where $\boldsymbol{M}$, $\boldsymbol{C}$, $\boldsymbol{K}$ are the 4×4 mass, damping and stiffness matrices, respectively; $\boldsymbol{x}(t)$ is the 4×1 displacement vector, $\boldsymbol{w}(t)$ is the 4×1 vector of external excitations induced by the guide rail deformations as expressed in Equations (1a)-(1c); $\boldsymbol{B}_1$ and $\boldsymbol{E}_1$ are 4×1 and 4×4 associated location matrices indicating the locations of control force and excitations, respectively.

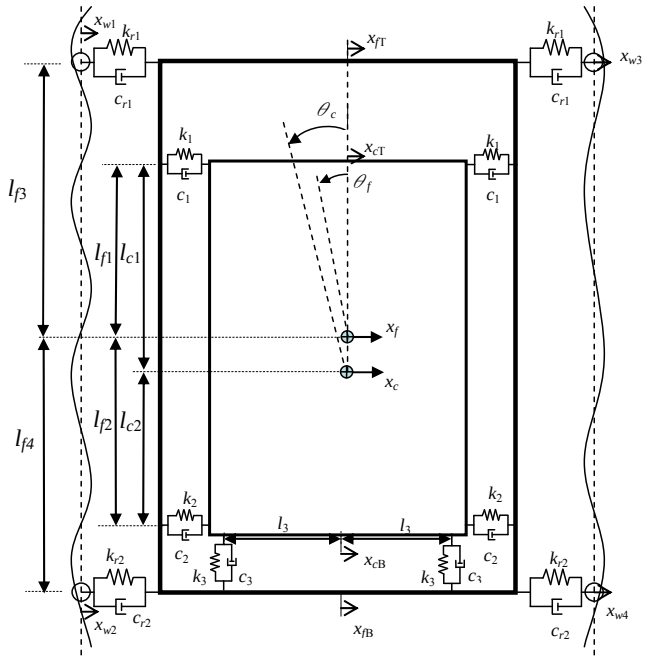

Fig. 3 Elevator Systems Modeled as four DOFs

Represented in state-space form, Equation (4) can be rewritten as

$$\dot{\boldsymbol{X}}(t) = \boldsymbol{A}\boldsymbol{X}(t) + \boldsymbol{B}\boldsymbol{u}(t) + \boldsymbol{E}\boldsymbol{w}(t) \tag{5}$$

where

$$\boldsymbol{X}(t) = \begin{Bmatrix} \boldsymbol{x}(t) \\ \dot{\boldsymbol{x}}(t) \end{Bmatrix}, \quad \boldsymbol{A} = \begin{bmatrix} \boldsymbol{0} & \boldsymbol{I} \\ -\boldsymbol{M}^{-1}\boldsymbol{K} & -\boldsymbol{M}^{-1}\boldsymbol{C} \end{bmatrix},$$
$$\boldsymbol{B} = \begin{bmatrix} \boldsymbol{0} \\ \boldsymbol{M}^{-1}\boldsymbol{B}_1 \end{bmatrix}, \quad \boldsymbol{E} = \begin{bmatrix} \boldsymbol{0} \\ \boldsymbol{M}^{-1}\boldsymbol{E}_1 \end{bmatrix}$$

are 8×1 state vector, 8×8 system matrix, 8×1 controller location matrix and 8×4 external excitation location matrix, respectively. Define a $p\times1$ control output vector $\boldsymbol{Z}(t)$ and an $s\times1$ output measurement vector $\boldsymbol{y}(t)$ as

$$\boldsymbol{Z}(t) = \boldsymbol{C}_1\boldsymbol{X}(t) + \boldsymbol{D}\boldsymbol{u}(t) \tag{6}$$

$$\boldsymbol{y}(t) = \boldsymbol{C}_2\boldsymbol{X}(t) \tag{7}$$

where $\boldsymbol{C}_1$, $\boldsymbol{D}$ and $\boldsymbol{C}_2$ are $p\times8$, $p\times1$ and $s\times8$ matrices. In the absence of time delay, the direct output feedback control force is calculated by

$$\boldsymbol{u}(t) = \boldsymbol{G}\,\boldsymbol{y}(t) \tag{8}$$

where $\boldsymbol{G}$ is a $1\times s$ time-invariant feedback gain matrix.

H_∞ CONTROL OF HIGH-SPEED ELEVATOR

H_∞ Direct Output Feedback Control Theory

According to H_∞ control algorithm [11], the H_∞ norm of transfer function matrix $\boldsymbol{T}_{\boldsymbol{Zw}}(j\omega)$ of control output with respect to external excitation takes the form

$$\left\|\boldsymbol{T}_{\boldsymbol{Zw}}(j\omega)\right\|_\infty = \sup\frac{\left\|\boldsymbol{Z}(j\omega)\right\|_2}{\left\|\boldsymbol{w}(j\omega)\right\|_2} < \gamma \tag{9}$$

where $j=\sqrt{-1}$, and sup is defined as the supremum over all $\boldsymbol{w}(t)$. γ is a positive attenuation constant which denotes a measure of control performance. Adopting a smaller value of γ means that more stringent performance of control system is required. From Eqs. (6)-(8), it is derived that the transfer function matrix $\boldsymbol{T}_{\boldsymbol{Zw}}(j\omega)$ is expressed by

$$\boldsymbol{T}_{\boldsymbol{Zw}}(j\omega) = (\boldsymbol{C}_1 + \boldsymbol{D}\boldsymbol{G}\boldsymbol{C}_2)[j\omega\cdot\boldsymbol{I} - (\boldsymbol{A} + \boldsymbol{B}\boldsymbol{G}\boldsymbol{C}_2)]^{-1}\boldsymbol{E} \tag{10}$$

Based on Eq. (9), the H_∞ norm of transfer function matrix $\boldsymbol{T}_{\boldsymbol{Zw}}(j\omega)$ satisfies the following constraint

$$\left\|\boldsymbol{T}_{\boldsymbol{Zw}}(j\omega)\right\|_\infty = \sup\bar{\sigma}[\boldsymbol{T}_{\boldsymbol{Zw}}(j\omega)] < \gamma \tag{11}$$

where sup $\bar{\sigma}$ is the largest singular value of $\boldsymbol{T}_{\boldsymbol{Zw}}(j\omega)$. It has been proved [11] that an optimal H_∞ control system is asymptotically stable if there exists a matrix $\boldsymbol{P}\geq0$ that satisfies the following Riccati equation

$$(\boldsymbol{A}+\boldsymbol{BGC}_2)^{\mathrm{T}}\boldsymbol{P}+\boldsymbol{P}(\boldsymbol{A}+\boldsymbol{BGC}_2) + \frac{1}{\gamma^2}\boldsymbol{PEE}^{T}\boldsymbol{P}+(\boldsymbol{C}_1+\boldsymbol{DGC}_2)^{\mathrm{T}}(\boldsymbol{C}_1+\boldsymbol{DGC}_2)=0 \quad (12)$$

One way to design the optimal H_∞ output feedback gain is to solve Eq. (12) with minimizing the Entropy of $\boldsymbol{T}_{\boldsymbol{Zw}}(j\omega)$ which takes the form [11]

$$E_n(\boldsymbol{T}_{\boldsymbol{Zw}},\gamma)=tr\{\boldsymbol{E}^{\mathrm{T}}\boldsymbol{PE}\} \quad (13)$$

where tr{-} denotes the trace of a square matrix. Then, the optimization problem to obtain gain matrix $\boldsymbol{G}$ is converted to minimize the Entropy in Eq. (13) subject to the constraint of Eq. (12). The Lagrangian L can be introduced as

$$L(\boldsymbol{G},\boldsymbol{P},\boldsymbol{\lambda})\equiv tr\Big\{\boldsymbol{E}^{\mathrm{T}}\boldsymbol{PE}+\boldsymbol{\lambda}[(\boldsymbol{A}+\boldsymbol{BGC}_2)^{T}\boldsymbol{P}+\boldsymbol{P}(\boldsymbol{A}+\boldsymbol{BGC}_2) + \frac{1}{\gamma^2}\boldsymbol{PEE}^{T}\boldsymbol{P}+(\boldsymbol{C}_1+\boldsymbol{DGC}_2)^{T}(\boldsymbol{C}_1+\boldsymbol{DGC}_2)]\Big\} \quad (14)$$

where λ is a 8×8 Lagrangian multiplier matrix. For simplicity and without loss of generality, let $\boldsymbol{D}^{\mathrm{T}}\boldsymbol{C}_1=\boldsymbol{0}$ and $\boldsymbol{D}^{\mathrm{T}}\boldsymbol{D}=\boldsymbol{I}$, the necessary and sufficient conditions for minimization of $L(\boldsymbol{G},\boldsymbol{P},\boldsymbol{\lambda})$ are derived and expressed by

$$\frac{\partial L}{\partial \boldsymbol{\lambda}}=(\boldsymbol{A}+\boldsymbol{BGC}_2)^{\mathrm{T}}\boldsymbol{P}+\boldsymbol{P}(\boldsymbol{A}+\boldsymbol{BGC}_2) + \frac{1}{\gamma^2}\boldsymbol{PEE}^{\mathrm{T}}\boldsymbol{P}+(\boldsymbol{C}_1+\boldsymbol{DGC}_2)^{\mathrm{T}}(\boldsymbol{C}_1+\boldsymbol{DGC}_2)=0 \quad (15a)$$

$$\frac{\partial L}{\partial \boldsymbol{P}}=(\boldsymbol{A}+\boldsymbol{BGC}_2+\frac{1}{\gamma^2}\boldsymbol{EE}^{\mathrm{T}}\boldsymbol{P})\boldsymbol{\lambda} + \boldsymbol{\lambda}(\boldsymbol{A}+\boldsymbol{BGC}_2+\frac{1}{\gamma^2}\boldsymbol{EE}^{\mathrm{T}}\boldsymbol{P})^{\mathrm{T}}+\boldsymbol{EE}^{\mathrm{T}}=0 \quad (15b)$$

$$\frac{\partial L}{\partial \boldsymbol{G}}=\boldsymbol{B}^{\mathrm{T}}\boldsymbol{P}\boldsymbol{\lambda}\boldsymbol{C}_2^{\mathrm{T}}+\boldsymbol{GC}_2\boldsymbol{\lambda}\boldsymbol{C}_2^{\mathrm{T}}=0 \quad (15c)$$

Thus, the procedures to obtain the H_∞ direct output feedback gain matrix $\boldsymbol{G}$ is: (i) to define a control output vector $\boldsymbol{Z}(t)$ of Eq. (6), (ii) to select the attenuation constant γ, and then (iii) to solve Eqs. (15a-15c) to obtain $\boldsymbol{P}$, $\boldsymbol{\lambda}$ and $\boldsymbol{G}$ by any iterative scheme..

Selection of Control Output

Define the control output vector satisfying $\boldsymbol{D}^{\mathrm{T}}\boldsymbol{C}_1=\boldsymbol{0}$ and $\boldsymbol{D}^{\mathrm{T}}\boldsymbol{D}=\boldsymbol{I}$ as

$$\boldsymbol{Z}(t)=\begin{bmatrix}\alpha\cdot\boldsymbol{\Gamma}\\ \boldsymbol{0}\end{bmatrix}\boldsymbol{X}(t)+\begin{bmatrix}\boldsymbol{0}\\ 1\end{bmatrix}\boldsymbol{u}(t)=\begin{bmatrix}\alpha\cdot m_p(\ddot{x}_c+l_{c2}\ddot{\theta})\\ \boldsymbol{u}(t)\end{bmatrix} \quad (16)$$

where $\boldsymbol{\Gamma}=m_p\cdot[1 \quad l_{c2} \quad 0 \quad 0]\left[-\boldsymbol{M}^{-1}\boldsymbol{K} \quad -\boldsymbol{M}^{-1}\boldsymbol{C}\right]$ to make $\boldsymbol{Z}(t)$ denote the combination of inertial force of passengers and control force. In Eq. (16), the control weighting factor, α, determines the relative importance between response reduction and control force requirement. When the control parameter γ is specified, it implies that the sum of passengers' inertial forces and control force should be limited to a level lower than γ. As $\boldsymbol{Z}(t)$ is reduced, the horizontal acceleration at the bottom of the car cabin $(\ddot{x}_c+l_{c2}\ddot{\theta})$ will become smaller. It has been proved [11] that under this constraint, the balance between reduction of passenger discomfort and limitation of control force is determined by the control weighting factor, α. Clearly speaking, the larger value of α, the more comfortable the passengers, but, the larger required control force $\boldsymbol{u}(t)$ of AMD. Once the control parameters γ and α were decided, one can compute the direct output feedback gain $\boldsymbol{G}$ by solving Eq. (15). $\alpha=0$ represents the uncontrolled case.

Selection of Optimum Control Parameters

For an AMD installed at the bottom of car cabin, $\boldsymbol{B}_1$ can be expressed as

$$\boldsymbol{B}_1=[1 \quad l_{c2} \quad 0 \quad 0]^{\mathrm{T}} \quad (17)$$

With reference to the study by Lin *et al*. [11], for a SDOF structure-AMD system, with total mass, m, original frequency, ω_0, and damping ratio, ξ_0, the analytical expression of optimal direct velocity feedback (DVF) $(\boldsymbol{C}_2=[0 \quad 0 \quad 0 \quad 0 \quad 1 \quad l_{c2} \quad 0 \quad 0])$ gain $\boldsymbol{G}$ is obtained from Eqs. (15a)-(15c) as

$$\boldsymbol{G}=-P_0\,P_{\mathrm{v}} \quad (18)$$

The controlled frequency, ω_c, and damping ratio, ξ_c, are expressed as

$$\omega_c=\omega_0 \ ; \qquad \xi_c=\xi_0+\frac{P_0^2}{P_1}\left(-\xi_0+\sqrt{\xi_0^2+\frac{P_1(P_2+2\alpha^2\cdot m_p^2\zeta_0^2\omega_0^2)}{\omega_0^2}}\right) \quad (19)$$

In above equations, m_p =mass of passengers, $P_0=\frac{1}{m}$,

$$P_1=P_0^2\left(1-\frac{1}{\gamma^2}\right),\ P_2=\gamma^2\omega_0^2m^2\left(1-\sqrt{1-\frac{\alpha^2m_p^2}{\gamma^2m^2}}\right),$$

$$P_v=\frac{-2\xi_0\omega_0+2\sqrt{\xi_0^2\omega_0^2+P_1(P_2+2\alpha^2\cdot m_p^2\xi_0^2\omega_0^2)}}{P_1},,$$

Under the constraints of P_2 and P_{v} to be real numbers, the selecting ranges of γ and α are confined in

$$0<\alpha\le\frac{m}{m_p}\gamma=\alpha_{ub,stable} \quad \text{when} \quad \gamma>\frac{\sqrt{1+8\xi_0^2+8\xi_0^4}}{4\xi_0^2+1} \quad (20a)$$

$$0<\alpha\le\frac{m}{m_p}\gamma\sqrt{1-\left(1+\frac{2\xi_0^2\omega_0^4}{P_1\gamma^2}\right)^2}=\alpha_{ub,stable} \quad \text{when} \quad \gamma\le\frac{\sqrt{1+8\xi_0^2+8\xi_0^4}}{4\xi_0^2+1} \quad (20b)$$

In addition, from Eq. (19) and Fig. 4, it is seen that the controlled damping ratio, ξ_c, can reach 100%. For a SDOF structure-AMD system, if a desired controlled damping ratio, ξ_c, is given, the required control weighting factor α_{ξ_c} can be obtained from Eq. (19) as

$$\alpha_{\xi_c}=\sqrt{\sqrt{\frac{-m^2\gamma^2[4m_p^2\xi_0^2(1-P_\alpha)-m_p^2]+m^2\gamma^2\sqrt{[4m_p^2\xi_0^2(1-P_\alpha)-m_p^2]^2-32m_p^4\xi_0^4P_\alpha(2-P_\alpha)}}{8m_p^4\xi_0^4}}} \quad (21)$$

where $P_\alpha=\frac{P_1}{P_0^2\gamma^2}(\xi_c-\xi_0)^2+\frac{2\zeta_0}{\gamma^2}(\xi_c-\xi_0)\cdot$

For the case of underdamping, $\xi_c\le 100\%$, the upper bound of α, $\alpha_{ub,cr}$, can also be obtained from Eq. (21). Consequently,

the optimum control strategy for an elevator system is (i) to define a control mode and control output $\boldsymbol{Z}(t)$ by Eq. (6), (ii) to select γ and $\alpha < \alpha_{ub,stable}$ for stable system based on Eqs. (20a) and (20b), (iii) to check $\alpha < \alpha_{ub,cr}$ from Eq. (21) for underdamping. Fig. 5 shows the design flow chart for optimum selection of control parameters α and γ.

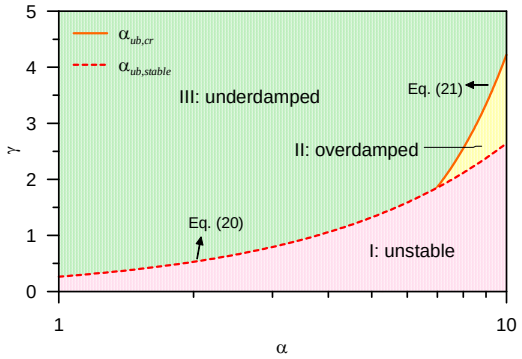

Fig. 4 Selection Range for Parameters of α and γ

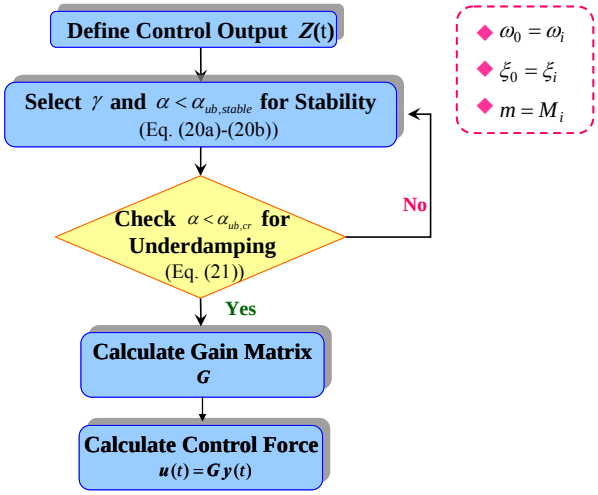

Fig. 5 Optimal Design Flow Chart for Selection of α and γ

NUMERICAL VERIFICATIONS

The elevator position function of time can be obtained from the elevator velocity curve during its operation. Substituting the position function into Eqs. (1a)-(1c), one can derive the time history of roller deformation. There is a fixed position difference between the upper roller and the lower roller at the same side of guide rail. This position difference will reflect a phase change in the externally applied forces on the upper and the lower roller. Thus, the external force vector $\boldsymbol{w}(t)$ can be computed by using the time history of the roller deformations, as shown in Fig. 6.

It is seen from Fig. 6 that the stepwise deformation of the guide rails plays the major role resulting in horizontal vibration of car cabin. Thus, it was considered as the external excitation in this study. For a full-scaled high-speed elevator system, its system parameters are listed in Table 1. Fig 7 shows the transfer functions of acceleration at the bottom of car cabin with respect to the external forces due to the upper and the lower roller deformation, respectively, without and with control of $\gamma = 4$ and $\alpha = 14$. Both acceleration transfer functions demonstrate an evident reduction in magnitude in response to the external forces. They also show the effectiveness of the feedback control on the first two modes.

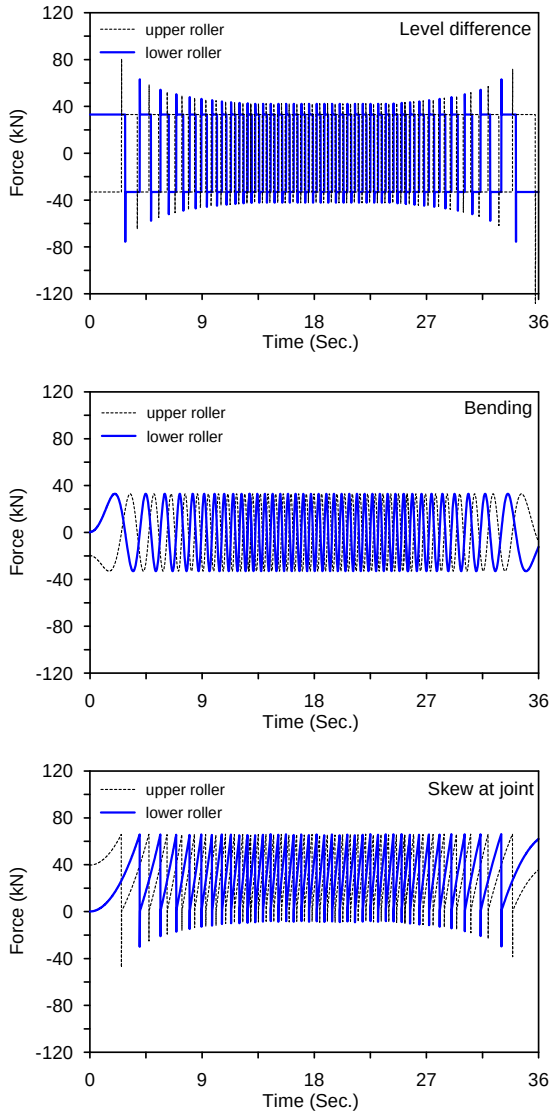

Fig. 6 Force Time Histories Due to (a) Level difference (b) Bending (c) Skew at joint of Guide Rails

The acceleration responses at the bottom of car cabin with and without control, and control force for the cases of $\gamma = 4$ and $\alpha = 14$ are shown in Fig. 8. It is seen that the peak acceleration response is reduced by 44% and less than 20 gal

satisfying the code requirement. The required maximum control force was only 1.3 % of the total weight of car cabin and passengers.

Table 1 Physical Parameters of Elevator Systems

m_c	1,200 kg	k_{r1}	33,000 N/m
m_f	2,100 kg	k_{r2}	33,000 N/m
I_c	2,270 kg . m^2	k_1	180,000 N/m
I_f	11,400 kg . m^2	k_2	1,000,000 N/m
m_p	70 kg	k_3	5,700,000 N/m
l_{c1}	1.6 m	c_{r1}	751.5 N . s/m
l_{c2}	1.5 m	c_{r2}	751.5 N . s/m
l_{f1}	1.45 m	c_1	3,822 N . s/m
l_{f2}	1.65 m	c_2	7,056 N . s/m
l_{f3}	3 m	c_3	39,200 N . s/m
l_{f4}	3 m	l_3	1 m

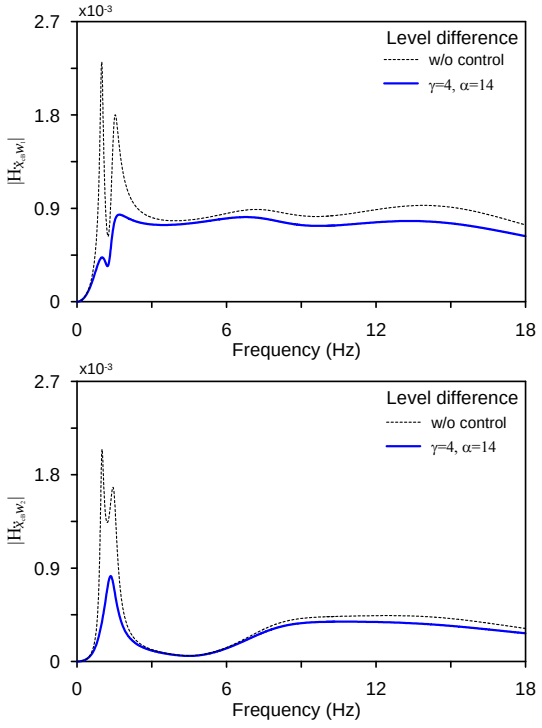

Fig. 7 Transfer Functions of Acceleration at the Bottom of Car Cabin with Respect to the External Forces due to (a) the Upper Roller (b) the Lower Roller.

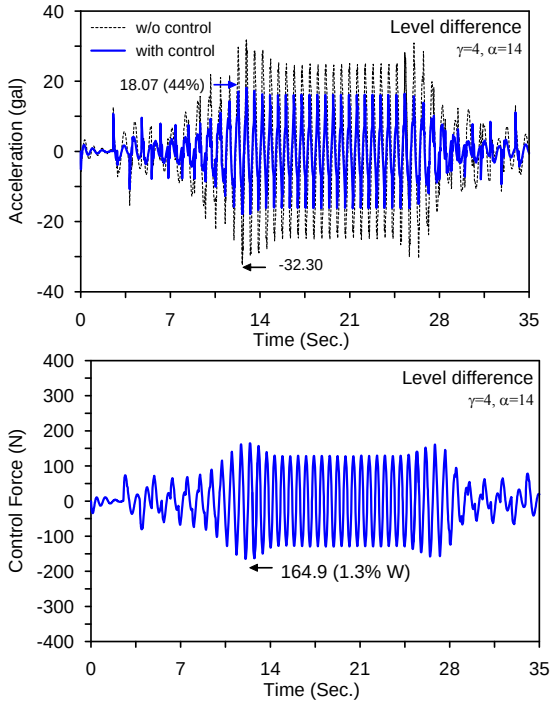

Fig. 8 Time Histories of Acceleration at the Bottom of Car Cabin with and without Control

CONCLUSIONS

This paper developed a four-degree-of-freedom dynamic model for characterizing the horizontal vibration behavior of high-speed elevator system. The proposed mathematical formulations for external force patterns have been shown to be useful in describing the guide rail deformations when the elevator is operating in high speed. Thus, an active control law can be designed for vibration reduction. This paper furthermore developed a H_∞ direct output feedback control strategy for a high-speed elevator equipped with an AMD control system. It has been testified to be effective along with the following conclusions:

1. The externally applied force due to the guide rail deformation has to do with the elevator traveling velocity as well as the guide rail length. Therefore, design of the car cabin system should take into account of the expected elevator traveling speed so as to avoid the fundamental frequency of the disturbance. Of the three external force patterns, the stepwise deformation of the guide rail plays the major role resulting in the horizontal vibration of passenger car.
2. One collocated AMD and velocity sensor are sufficient and effective in reducing the acceleration in passenger car based on the developed H_∞ direct output feedback control algorithm. A design flowchart was proposed to select optimum control parameters of γ and α to assure system stability and control efficiency. Finally, a full-scaled high-speed elevator system was demonstrated to prove the applicability and control effectiveness of the proposed AMD system.

REFERENCES

[1] Mizuguchi, H., Nakagawa, T., Fujita,Y., (2005), "High-Speed Elevators in Taipei 101", *Elevator World*, **9**, pp. 71-76.

[2] Feng, Y.H., Zhang, J.W., (2007), "Study on Active Control Strategy of Horizontal Vibrations of High-speed Elevator", *Journal of System Simulation*, Vol. **19**, No. 4, pp. 843-845.

[3] Liao, X.B., Fu, W.J., Zhu, C.M., (2003), "The Experiment System and Simulation for the Active Control of Lateral Vibration of Elevator", *Machine Design and Research*, Vol. **19,** No. 6, pp. 65-67.

[4] Fu, W.J., Zhu, C.M., Zhang, C.Y., (2005), "Modeling and Simulation for Dynamics of Single Wrapped Elevator", *Journal of System Simulation*, Vol. **17**, No. 3, pp. 635-638.

[5] Fu, W.J., Liao, X.B., Zhu, C.M., (2005), "Structural Optimization to Suppress Elevator Horizontal Vibration Using Virtual Prototype", *Journal of System Simulation*, Vol. 17, No. 6, pp. 1500-1504.

[6] Li, L.J., Li, X.F., Zhang, G.X., Li, Z., (2002), "Horizontal Vibration Model of Elevator Car", *Hoisting and Conveying Machinery*, No. 5, pp. 3-5.

[7] Li, X.F., Zhang, C.Y., Li, L.J., Zhang, G.X., Guo, L.F., (2005), "Influences of Elevator Guide Rail on the Cabin Vibration", *China Mechanical Engineering*, Vol. 16, No. 2, pp. 115-122.

[8] Okamoto, K.I., Yumura, T., Kuraoka, H., Saragai, K., Kojima, K., (2000), "A New Slide Guide Shoe to Suppress Elevator Vibration ", *Proceedings of Elevator*, Japan.

[9] Utsunomiya, K., Okamoto, K., Yumura, T., Sakuma, Y., (2006), "Vibration Control of High-Speed Elevators Taking Account of Electricity Consumption Reduction", *Transactions of the Japan Society of Mechanical Engineers. C*, Vol.**72**, No.719, pp. 2048-2055.

[10] Skalski, C.A., (2005), "Active Vibration Control for Elevators", *IEEE CT Mini-Conference, Control Systems – Theory and Applications.*

[11] Lin, C.C., Chang, C.C. Chen, H.L., (2006), "Optimal H_∞ Output Feedback Control System with Time Delay", *Journal of Engineering Mechanics*, ASCE, Vol. **132**, No.10, 1096-1105.